

**Summary** This paper describes theoretical modelling and experimental measurements of the wall temperatures in the corners of buildings. A dimensionless cold bridge temperature (DCBT) is proposed as a parameter to characterise cold bridges. A simple resistance model is suggested as an improved method for calculating cold bridge temperatures in corners. This model shows reasonable agreement with both finite-element modelling and measured data. Theoretical studies suggest that an increased internal surface resistance at the corner results in a substantial increase in cold bridging. During transient conditions the DCBT can vary by 50%. The impact of external corners on the risk of mould growth is discussed. Mean internal relative humidities lower than the normally accepted value of 70% are suggested for rooms with significant cold bridges.

## Cold bridging at corners: Surface temperature and condensation risk

T ORESZCZYN BSc PhD

Research in Building Group, Polytechnic of Central London, 35 Marylebone Road, London NW1 5LS, UK

Received 4 March 1988, in final form 8 July 1988

### List of symbols

$d$	Wall thickness (m)
DCBT	Dimensionless cold bridge temperature
DR	Dimensionless resistance
$h$	Surface heat transfer coefficient ( $\text{W m}^{-2} \text{K}^{-1}$ )
$\lambda$	Thermal conductivity ( $\text{W m}^{-1} \text{K}^{-1}$ )
$n$	Dimension
$R$	Thermal resistance ( $\text{m}^2 \text{K W}^{-1}$ )
$T$	Temperature ( $^{\circ}\text{C}$ )
$U$	One dimensional $U$ -value i.e. $1/(1/R_{si} + k/d + 1/R_{so})$ ( $\text{W m}^{-2} \text{K}^{-1}$ )

### Subscripts

cb	Cold bridge
1	One dimensional
i	Inside
o	Outside
s	Surface
window	Window
wall	Wall

### 1 Introduction

Condensation is a major problem in a large number of dwellings in the UK causing an estimated 1.5 million cases of severe dampness<sup>(1)</sup>. The corner of the room is one of the most common sites for surface condensation and mould growth. This is because inside surface temperatures are lower at corners than for a plain wall for the following reasons:

- The construction of a corner involves a cold bridge. Even if the corner is constructed from the same material as the wall a cold bridge exists because of two-dimensional heat flow.
- At external corners of buildings air flow may cool the corners more than at the plain wall.
- Internally, air movement may be less in corners reducing the heat and moisture transfer particularly if the corner is obstructed with furniture.

This paper concerns itself primarily with reason (a); cold bridging due to the construction of the corner.

A cold bridge occurs when the external leaf of the building is penetrated by a region of lower thermal resistance. A corner is defined in this paper as the meeting of two or

three mutually perpendicular plane *external* surfaces. A two-dimensional (2D) corner occurs where two external walls or an external wall and roof join. A three-dimensional (3D) corner occurs when two external walls and a roof or ground floor meet.

Many papers and reports<sup>(2-6)</sup> show the effect of cold bridging on the surface temperature of corners and advise designers to consider carefully their affect on the risk of condensation. Methods employed to assess corner cold bridges are:

- Experimental
- Analogue simulation (e.g. Reference X)
- Digital (e.g. finite difference (resistance networks and relaxation method), finite element)

Analytic solutions are available for corners<sup>(7)</sup> but they assume that the surfaces are maintained at a constant temperature and hence zero surface resistance. Although fairly accurate in calculating heat flow<sup>(8)</sup>, this method cannot be used to calculate corner temperatures. Other methods used for cold bridges, such as the proportional area method<sup>(2)</sup>, assume one-dimensional heat flow and so are inappropriate for corners.

The above methods are time consuming and thus unavailable to the average building designer. In addition, the results published so far have not been in a form useful to building designers.

This paper examines the reduction in surface temperature in external corners using a finite-element package, an easy-to-use resistance model and measured data.

### 2 Modelling

#### 2.1 Finite element

PAFEC<sup>(9)</sup>, a commercial three-dimensional finite element (FE) package has been used to model the heat flow through various corner constructions.

To check the correct operation of the FE model, comparisons between other published results of two-dimensional heat flow were made for a lintel<sup>(10)</sup> and corner<sup>(11,12)</sup>. The results showed close agreement (i.e. within  $0.1^{\circ}\text{C}$ ).

Figure 1 shows temperature contours for three 2D corners, a solid brick and a cavity wall, both with and without insulation. These computer simulations assume an outside

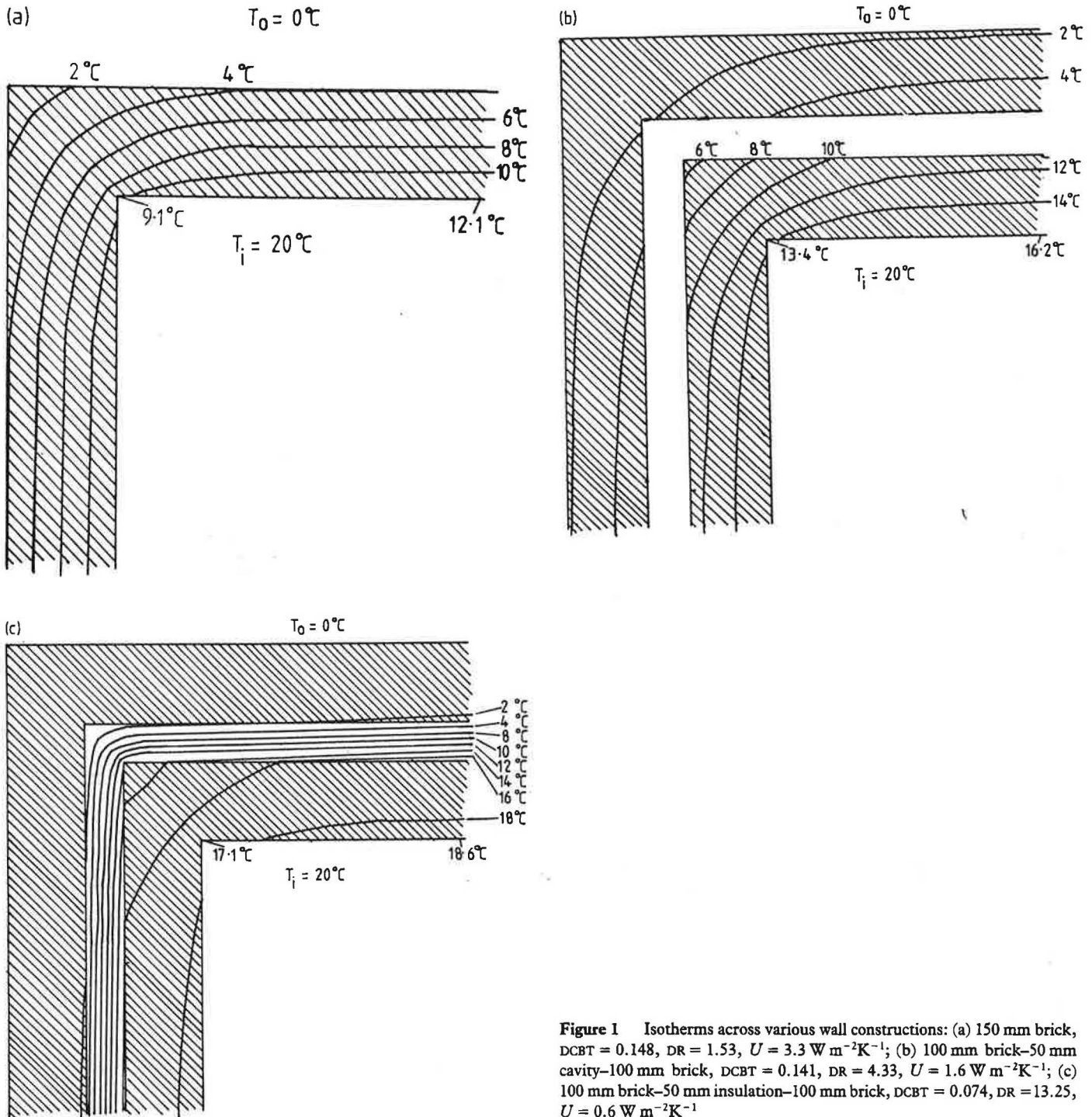


**Figure 1** Isotherms across various wall constructions: (a) 150 mm brick, DCBT = 0.148, DR = 1.53,  $U = 3.3 \text{ W m}^{-2}\text{K}^{-1}$ ; (b) 100 mm brick–50 mm cavity–100 mm brick, DCBT = 0.141, DR = 4.33,  $U = 1.6 \text{ W m}^{-2}\text{K}^{-1}$ ; (c) 100 mm brick–50 mm insulation–100 mm brick, DCBT = 0.074, DR = 13.25,  $U = 0.6 \text{ W m}^{-2}\text{K}^{-1}$

temperature of  $0^\circ\text{C}$  and inside temperature of  $20^\circ\text{C}$ . Constant heat transfer coefficients<sup>(2)</sup> have been used along internal, external and cavity surfaces ( $R_{si} = 0.12 \text{ m}^2\text{K W}^{-1}$  and  $R_{so} = 0.06 \text{ m}^2\text{K W}^{-1}$ ) as have the thermal conductivities of the materials.

As the wall is progressively insulated, the internal surface temperature of the wall increases at the corner and along the wall surface. The temperature at the corner can be characterised by relating it to the easy-to-calculate temperature of the plain wall where one-dimensional heat flow occurs, i.e. at a distance greater than 0.5 m from the corner. The plain wall (one-dimensional) temperature can then be calculated using the standard  $U$ -value calculation<sup>(2)</sup>. The temperature difference between the corner and the plain wall is a function of the inside and outside air temperature.

The author therefore proposes to define a dimensionless cold bridge temperature (DCBT) as the temperature difference between the coldest spot at the cold bridge on the internal surface ( $T_{cb}$ ) and the coldest location where one-dimensional heat flow occurs ( $T_i$ ), divided by the temperature difference between the inside and outside of the house:

$$\text{DCBT} = \frac{T_i - T_{cb}}{T_i - T_o} \quad (1)$$

The higher the DCBT the more severe the cold bridge. For example, typical values for a cold bridge located in a single skin brick wall are given in Table 1.

The DCBT is not only a function of the details of construction and the thermal characteristics of the material, but also the

Table 1

Configuration	DCBT
2D corner	0.15
3D corner	0.25
Concrete floor slab joining a wall	0.03
Concrete floor slab extending as a balcony	0.20
Window reveal	0.15

internal heat transfer coefficients and to a lesser extent the external heat transfer coefficient (in a similar way to a  $U$ -value).

Figure 1 shows that as a wall is progressively insulated, the internal surface temperature at a corner increases and the cold bridging decreases, i.e. the DCBT decreases.

Figure 2 shows that the cold bridging in the corner is limited to a small area, with 90% of the temperature difference occurring in the first 18 cm from the corner. This is in agreement with the small areas normally associated with mould growth in corners. As a rough rule, one-dimensional heat flow may be assumed at distances greater than five times the thickness of the wall from the corner for walls typical in the UK.

## 2.2 Resistance

Finite element packages such as PAFEC are too complex for designers to use. A simplified thermal model of a corner cold bridge is now presented, based on a simple thermal resistance circuit shown in Figure 3. For two adjoining walls of the same material, and assuming the same  $R_{si}$  at the corner as for the rest of the wall, the DCBT can be calculated from the following equation, which has been derived from the resistance network shown in Figure 3:

$$DCBT(n) = \frac{n}{DR + n} - \frac{1}{DR + 1} \quad (2)$$

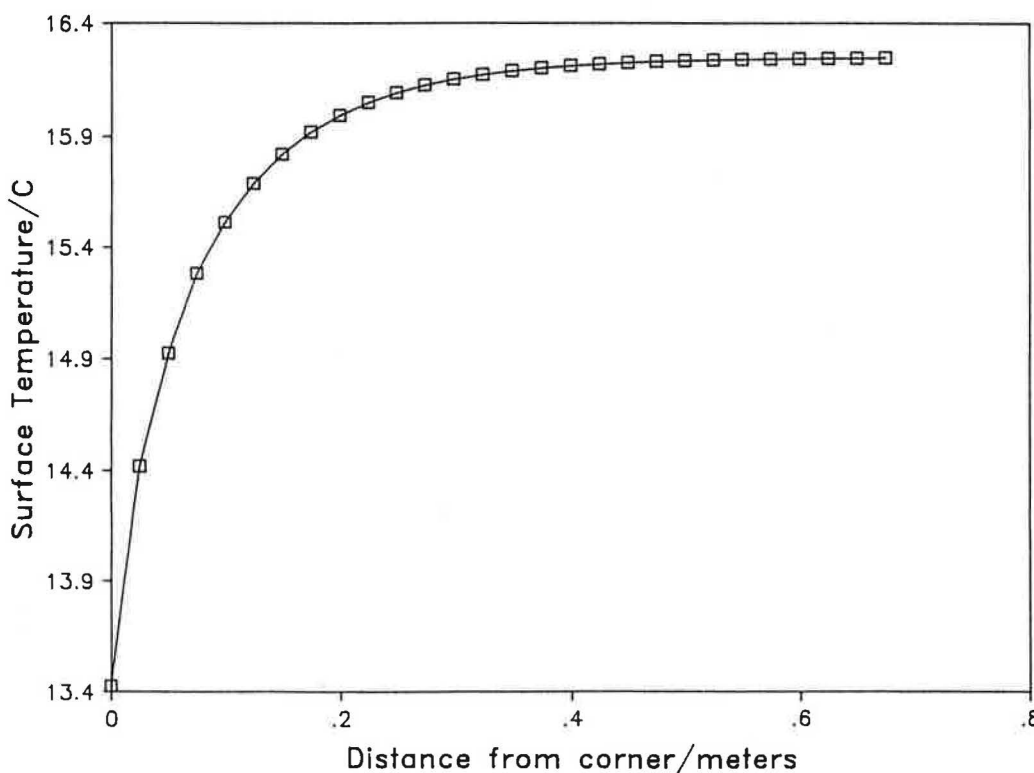


Figure 2 Computed temperature distribution along the inside surface of a 100 mm brick-50 mm cavity-100 mm brick wall corner

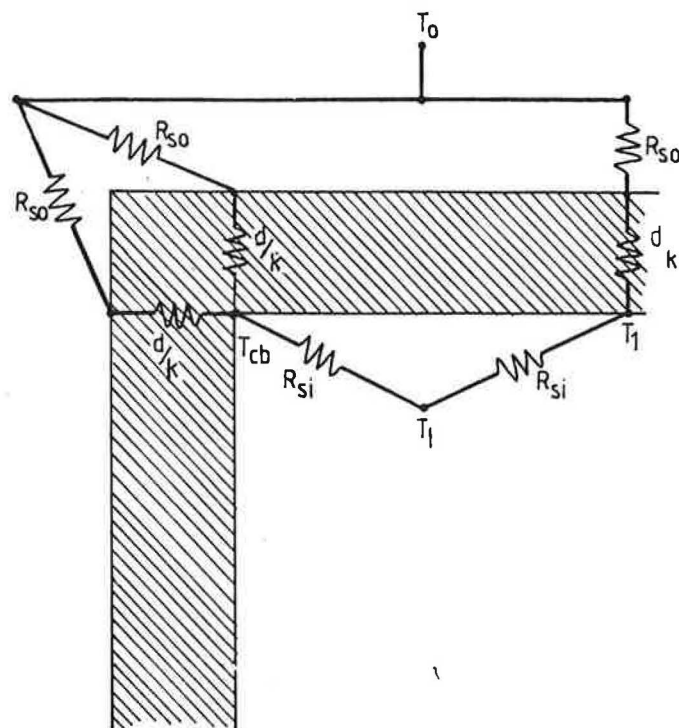


Figure 3 Resistance model for two-dimensional corner of homogeneous material:  $DCBT = (T_1 - T_{cb}) / (T_1 - T_0)$ . For 2D corner  $DCBT = [2/(DR + 2)] - [1/(DR + 1)]$  where  $DR = (d/K + R_{so})/R_{si}$ .

where  $n$  is the dimension (2 for a 2D corner and 3 for a 3D corner) and  $DR$  is the dimensionless resistance:

$$DR = \frac{d/\lambda + R_{so}}{R_{si}} \text{ or } \frac{1/U - R_{si}}{R_{si}} \quad (3)$$

Figure 4 is a graph of DCBT versus  $DR$  for a 2D and 3D corner. As the level of insulation increases the cold bridging decreases, except for highly conductive walls. For comparison, Figure 4 shows the effective DCBT

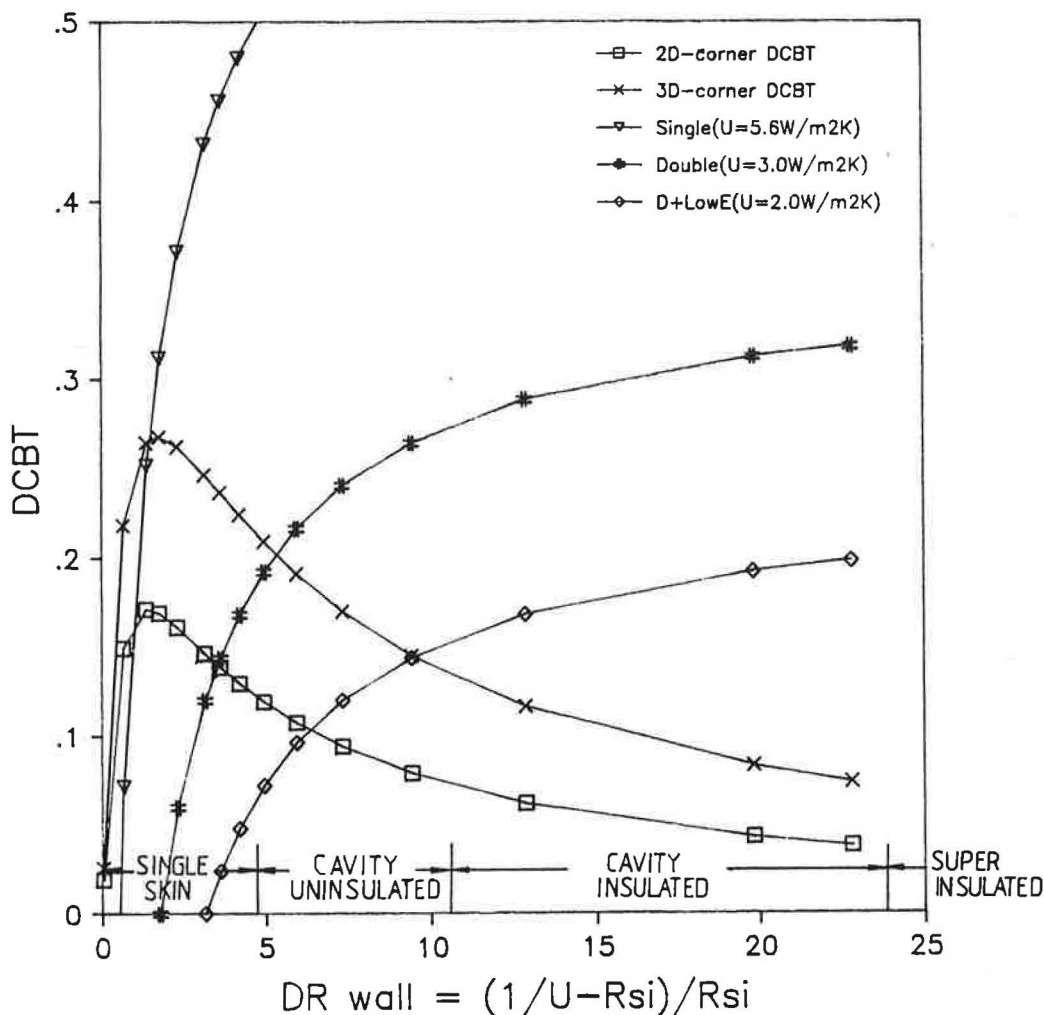


Figure 4 DCBT for various walls with two- and three-dimensional corners and windows as predicted by a simple resistance model

$(T_{wall} - T_{window}/(T_i - T_o))$  due to various types of glazing installed in walls of differing  $U$ -value.

$$DCBT_{window} = (U_{window} - U_{wall})R_{si} \quad (4)$$

or

$$DCBT_{window} = U_{window} R_{si} - \frac{1}{DR_{wall} + 1} \quad (5)$$

Contrary to what happens in corners, as the wall is insulated the cold bridging increases. This is because the wall temperature increases with insulation but the window temperature remains constant regardless of the level of insulation in the wall.

Note that the DCBT for a 3D corner is higher than that for double glazing if the wall is not insulated. Therefore, in rooms with two exposed walls and an exposed ceiling the temperature in the corner may be lower than that of a double glazed window. This highlights the need to insulate walls if double glazing is to be installed in rooms with external 3D corners and condensation problems.

Figure 5 compares the simple resistance model with results obtained using the FE model. The squares correspond to finite element calculations for various wall constructions (Table 2). Included in Table 2 and on Figure 5 are results from the Building Research Station in England and Denmark<sup>(8)</sup>. These were obtained using the relaxation method and a resistance network analyser. The crosses correspond to the same construction but with the DCBT calculated using the resistance model (equation 2). The

resistance model is in very close agreement with the finite-element model over the range normally experienced for external walls. The triangular points plotted on Figure 5 correspond to the predicted DCBT for the same wall constructions using the German practice documented by Erich Schield<sup>(13)</sup>. This assumes that the internal surface resistance at a corner is three times the normal value (i.e. 0.36 rather than 0.12 m<sup>2</sup>K W<sup>-1</sup>) and that the external surface resistance is zero at the corner. The resistance model is a much better fit to the FE model than the German practice, particularly for single skin uninsulated walls.

The main shortcoming of the resistance model is that the DCBT it predicts is independent of the location of the insulation within the wall, i.e. as long as the wall has the same  $U$ -value the DCBT predicted by the resistance model is the same regardless of whether the wall is drylined or externally clad. This shortcoming also applies to the German practice. Finite element modelling shows that the location of the insulation can change the DCBT by up to 0.05 (Table 3). The further the insulation is from the internal surface the smaller the DCBT for a wall of the same  $U$ -value, although Sarkis and Letherman<sup>(12)</sup> have reported modelled results where this is not the case. Thus external cladding gives the lowest steady-state DCBT. However, in terms of energy loss it is more beneficial to locate insulation near the inside of the wall<sup>(12)</sup>.

Under some circumstances it may be beneficial to reduce cold bridging by introducing high thermal conductivity materials at corners and thus allowing heat to be conducted

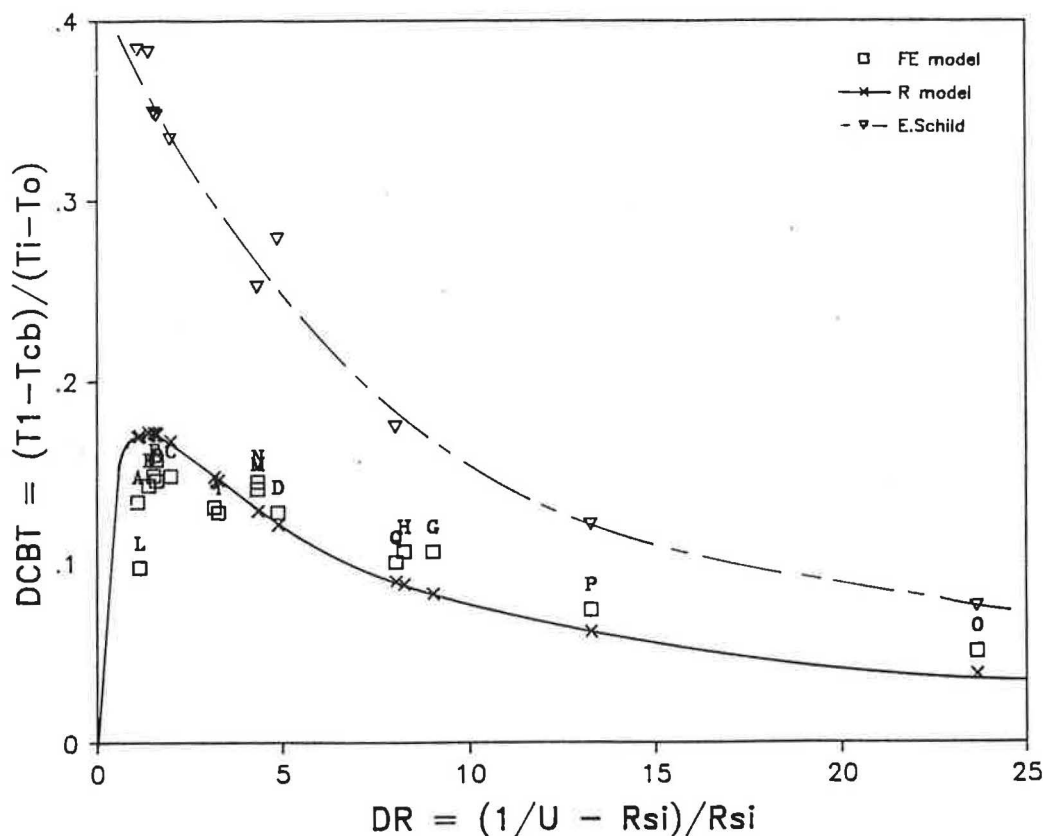


Figure 5 Comparison of modelled DCBT from three different models, finite element, resistance and Schild's<sup>(13)</sup> (See Table 2 for key to FE model.)

from the middle of the wall to the corner. For example, adding 5 mm of metal to the inside corner of a 105 mm brick wall reduces the DCBT from 0.15 to 0.04, according to FE modelling.

### 3 Internal heat transfer

Both FE and resistance modelling show the DCBT to be sensitive to changes in  $h_{si}$ . For example, the DCBT for a cavity wall is 0.148 for  $h_{si} = 6 \text{ W m}^{-2}\text{K}^{-1}$  compared with 0.138 for  $8 \text{ W m}^{-2}\text{K}^{-1}$ , with an even greater variation for single-skin walls—the greater variation at smaller values of DR is a

consequence of the steeper gradient at lower DR (see Figure 4).

The external heat transfer coefficient is less important; a change in  $R_{so}$  from 0.06 to  $0.03 \text{ W m}^{-2}\text{K}^{-1}$  only results in a 1% change in DCBT.

The DCBT is also sensitive to variations in  $h_{si}$  along the internal surface. All the preceding analysis has assumed the same  $h_{si}$  in the corner as in the middle of the wall. Gertis<sup>(14)</sup> suggests the internal surface heat transfer coefficients given in Table 4.

This variation is a result of reduced air movement in the

Table 2 Modelled DCBT for various corners using finite-element and finite difference models (plus key to Figure 5)

Serial	Description	$k(\text{W m}^{-1}\text{K}^{-1})$	$d(\text{mm})$	DR	DCBT	$U\text{-value}$
A	Single leaf, dense concrete	1.40	100	1.10	0.134	3.98
B	Single leaf, floor grade concrete	1.13	150	1.61	0.146	3.19
C	Single leaf, brick	0.84	150	1.99	0.148	2.79
D	Single leaf, lightweight concrete	0.19	100	4.88	0.128	1.42
E	Single leaf, dense concrete	1.40	150	1.39	0.143	3.48
F	Single leaf, brick	0.84	105	1.53	0.148	3.27
G	Single leaf, gas concrete <sup>(8)</sup>	0.28	355	9.03	0.106	0.738
H	Single leaf <sup>(8)</sup>	0.21	203	8.26	0.106	0.9
I	Single leaf, brick <sup>(8)</sup>	0.81	355	3.28	0.128	1.6
J	Single leaf <sup>(8)</sup>	0.58	203	3.17	0.131	2.0
K	Single leaf <sup>(8)</sup>	1.44	203	1.60	0.157	3.2
L	Single leaf <sup>(8)</sup>	2.48	203	1.14	0.097	3.9
M	Cavity wall with 50 mm airgap		250	4.33	0.141	1.56
N	Cavity wall with 100 mm air gap		300	4.33	0.145	1.56
O	Cavity wall with 100 mm insulation		300	23.67	0.051	0.34
P	Cavity wall with 50 mm insulation		250	13.25	0.074	0.58
Q	Cavity wall with 25 mm insulation		225	8.04	0.100	0.92



**Table 3** DCBT for walls with similar  $U$ -value but different location of insulation

	DR	$U$ -value ( $\text{W m}^{-2}\text{K}^{-1}$ )	DCBT	
			$R$ model	FE model
Single leaf brick wall drylined	11.9	0.64	0.07	0.12
Single leaf brick wall externally clad	11.9	0.64	0.07	0.07
Cavity wall with insulation	13.2	0.58	0.06	0.07

corner causing a smaller convective heat transfer coefficient, and a reduced radiative coefficient as a result of the changing view factor. Nevander<sup>(15)</sup> suggests that the radiative coefficient at the corner of a wall can drop by 50% compared with that at the mid wall. However, modelling the radiative heat transfer in corners is made difficult because the surface emissivity of walls drops at the low angles of incidence which dominate the view factor close to the corner.

To calculate how significant any variation in the internal surface heat transfer coefficient is likely to be, four different variations of heat transfer coefficient were examined using the FE model (Figure 6). Changing  $h_{si}$  from a constant  $8.3 \text{ W m}^{-2}\text{K}^{-1}$  to  $4 \text{ W m}^{-2}\text{K}^{-1}$  in the corner results in the DCBT increasing from 0.148 to 0.240. This is a 60% increase in DCBT. The accurate prediction of cold bridging in corners is therefore critically dependent on the heat transfer coefficient in a corner.

#### 4 Measurements

To test the accuracy of FE modelling at predicting corner surface temperatures in buildings, measurements were carried out in a north facing single-storey bathroom with two external walls and a roof, i.e. both a 2D and 3D corner.

Because the bathroom was facing north and overshadowed the corner received no direct sunlight and so minimal solar gains. The bathroom was also in a location sheltered from the wind by the surrounding land.

The walls consisted of 105 mm brick, 50 mm cavity, 105 mm brick and 13 mm of plaster ( $U = 1.4 \text{ W m}^{-2}\text{K}^{-1}$ ). The roof was flat with 3 mm cork tiles, 10 mm plasterboard, 25 mm insulation, an airspace, 18 mm chipboard and a 19 mm bitumen felt layer ( $U = 0.8 \text{ W m}^{-2}\text{K}^{-1}$ ).

Surface wall and air temperatures were monitored at several locations both inside and outside the room over a period of several days, using thermocouples and a datalogger.

Care was taken to place thermocouple wires along anticipated thermal contours, thus preventing any thermal bridging due to the wires.

Figure 7 shows the measured DCBT over a period of 3 days during which the room was heated by a fan heater controlled by a thermostat ( $T_i = 26^\circ\text{C}$  to  $30^\circ\text{C}$ ). During the measuring

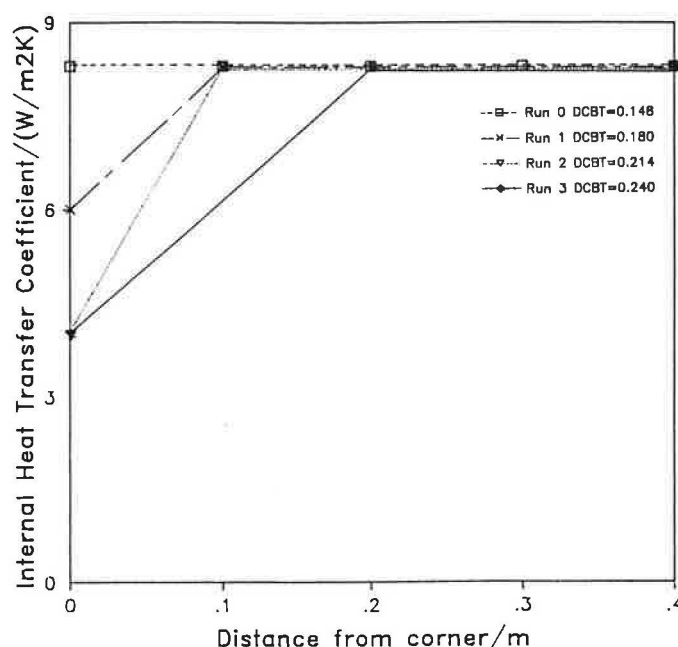
period the outside temperature fluctuated between  $0^\circ\text{C}$  and  $20^\circ\text{C}$ . Errors in measuring the DCBT were small ( $\approx \pm 7\%$ ) despite the relatively small temperature differences. This is because differential temperature measurements were made with thermocouples instead of less accurate absolute measurements. This is an advantage of quoting the DCBT for experimental results instead of absolute temperatures.

Comparisons of measured data with modelled steady-state DCBT is made difficult for the following reasons:

- Variations in outside temperature cause the DCBT to vary.
- Material properties and heat transfer coefficients are difficult to predict accurately (section 3).

Measurements of the convective internal heat transfer coefficient were made using a transient method developed by Yaneske and Forrest<sup>(16)</sup>. The measured internal convective heat transfer coefficient was  $7.1 \text{ W m}^{-2}\text{K}^{-1}$  compared with  $3 \text{ W m}^{-2}\text{K}^{-1}$  the standard CIBSE value<sup>(2)</sup>. A value of  $7.1 \text{ W m}^{-2}\text{K}^{-1}$  corresponds to air at  $1.5 \text{ m s}^{-1}$  according to CIBSE Guide Section C3. Measured surface velocities near the wall were  $0.6 \text{ m s}^{-1}$ .

To determine the radiative coefficient the internal wall surface temperatures were measured and found to be nearly the same as the temperature at the middle of the external wall temperature, therefore the radiative transfer to the plain section of the wall can be assumed negligible.

**Figure 6** Internal heat transfer coefficient along the surface of a brick cavity wall corner and the resulting DCBT**Table 4** Internal surface heat transfer coefficients ( $\text{W m}^{-2}\text{K}^{-1}$ )

Configuration	Value
Undisturbed free vertical surfaces	8
Corner, no furniture	6
Corner, behind furniture	4

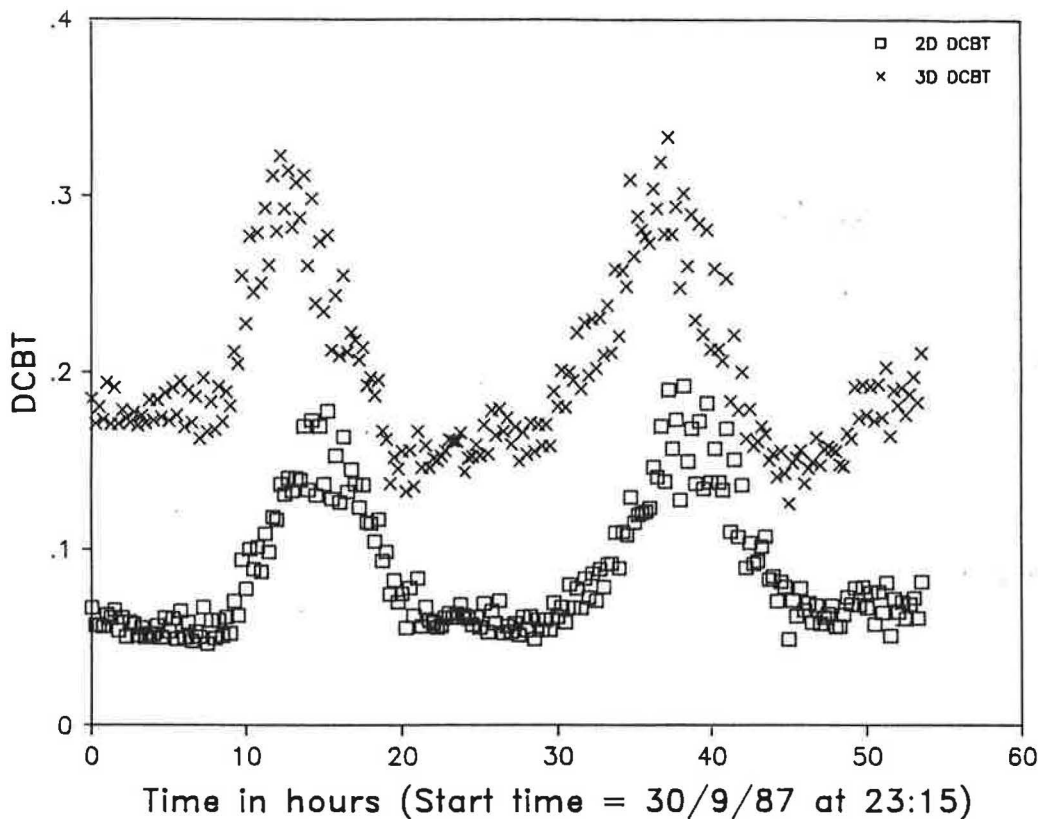


Figure 7 Measured DCBT at the corner of a cavity wall (2D corner) and the corner of a brick cavity wall and ceiling (3D corner)

## 5 Transients

Figure 7 shows the measured variation in DCBT due to fluctuations in external air temperature. Clearly the DCBT changes with external air temperature and any comparison between modelled and measured data must involve the use of a transient model for all but the few days in the year when day and night air temperatures remain constant.

FE modelling was used to produce transient data for one day's measured inside ( $25^{\circ}\text{C}$  to  $27^{\circ}\text{C}$ ) and outside temperatures ( $5^{\circ}\text{C}$  to  $13^{\circ}\text{C}$ ). Figure 8 compares the measured and modelled results. Clearly there is good agreement in the transient nature of the model. However, the modelled DCBT appears to be consistently 15% higher than measured (Figure 8(a)). Some of this discrepancy can be attributed to the accuracy of the equipment (7%) and some to the ther-

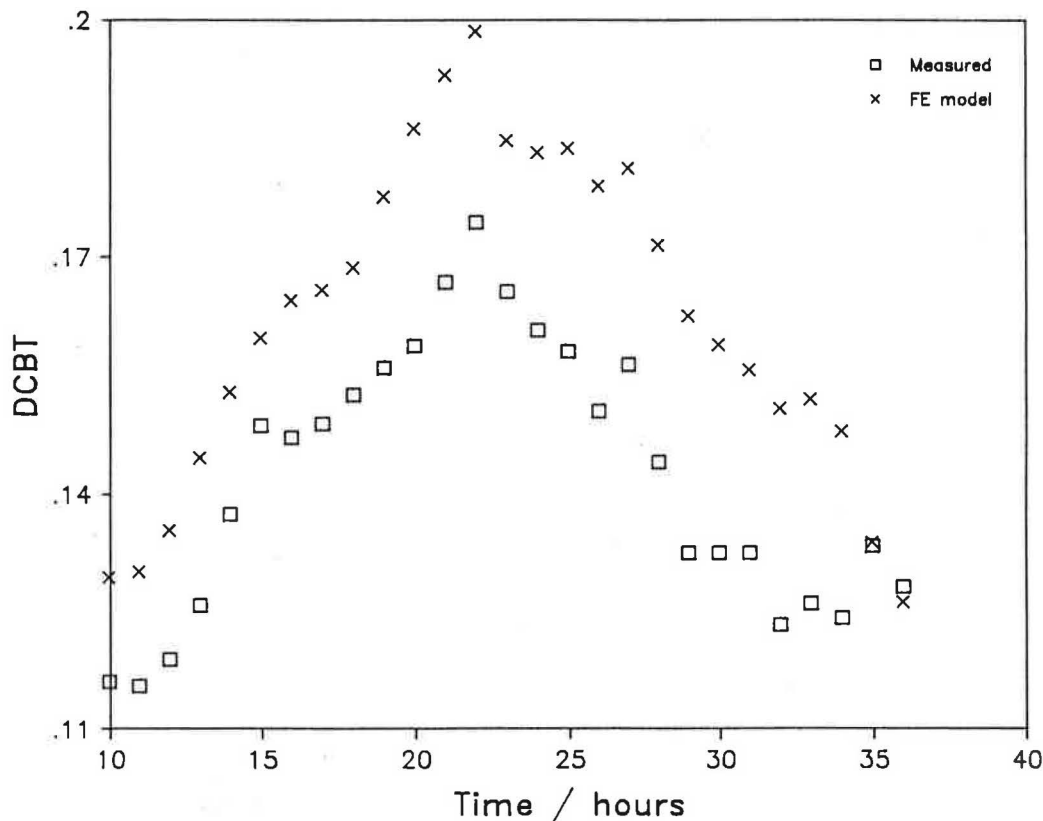


Figure 8 Measured and modelled (FE) DCBT at the same corner as Figure 7

mocouples not being located exactly at the corner. A displacement of 1 cm would be required to account for this fully. A reduced heat transfer coefficient in the corner would result in a modelled DCBT being lower and not higher than measured, since the modelled data assumes uniform  $h_{si}$  along the surface. This result suggests that there is no difference between the corner and mid-wall heat transfer coefficient. One possible source for the discrepancy is the mixing of air along the cavity. The FE model assumes that the cavity is filled with a solid material whose thermal properties are similar to those of air in a cavity and not a real fluid. Hence mixing cannot be accounted for by the FE model.

The transient nature of the real data, although a nuisance while monitoring, is an important effect in buildings and means that the DCBT can increase by 25–50% during the measurement as a result of external transients (i.e. even with constant internal temperatures). This variation will be important in the formation of condensation at cold bridges. As the external temperature increases the external vapour pressure in the atmosphere increases at the same time as the DCBT increases.

## 6 Cold bridging and mould growth

Measurements in environmental chambers have shown that mould grows on most wall covering materials if the relative humidity is greater than 80% for a period of several days<sup>(17)</sup>. It should be noted that surface condensation is not required to trigger the growth of mould<sup>(18)</sup>.

The relative humidity at the corner of a room will depend on the air temperature and vapour pressure at the corner. If a constant vapour pressure is assumed throughout the room, psychrometric data<sup>(2)</sup> can be used to calculate the relative humidity in the main bulk of the room (i.e. the air at  $T_i$ ), relative to that at the surface for any DCBT. Figure 9 shows

the humidity in the centre of the room when the RH is 80% at the surface of the cold bridge for various cold bridges. This is done for four separate wall constructions. All walls with  $U$ -values less than  $1.2 \text{ W m}^{-2}\text{K}^{-1}$  and with no cold bridges (DCBT = 0), will not get mould growth (local RH > 80%), provided the room humidity is kept below 70%. This is in agreement with Reference 4 which asserts that a condensation risk will be unacceptably high when the mean internal relative humidity exceeds 70%. However, if the wall has a 2D corner (Figure 9 has plotted the DCBT for a 2D corner), only insulated walls ( $U < 0.6 \text{ W m}^{-2}\text{K}^{-1}$ ) will remain mould free at RHs up to 70%. Therefore, to prevent mould occurring at uninsulated walls with 2D corners, the relative humidity in the bulk of the room may need to be kept below 55%.

Figure 9 can, therefore, be used to calculate the maximum humidity for any given cold bridge provided its DCBT is known. For example, the 2D DCBT at a corner where a filled cavity meets a flat insulated concrete roof with concrete downstand is 0.3, and 0.45 for the same 3D corner. The humidity in this room must be maintained below 55% to prevent mould growth on the 2D corner and below 48% to prevent mould growth at the 3D corner. Maintaining such low humidities in a room can prove very difficult. Figure 10 shows how the mean internal relative humidity (over the heating season) varies with total space heating load (the sum of the loads in zone 1 and zone 2) as predicted by a combined thermal and condensation model<sup>(19)</sup>. Zone 1 is the living room and zone 2 the remainder of the dwelling. If we assume that the flat has no cold bridges,  $27 \text{ GJ y}^{-1}$  of space heating is required to maintain an RH of less than 70% in both zones. Thus the space heating would cost £130, i.e. a mean internal temperature of  $12^\circ\text{C}$  in zone 2. If however, the building has a cold bridge with DCBT = 0.3 the mean relative humidity must be kept below 55% to prevent mould growth. This would require a mean internal temperature of  $15.8^\circ\text{C}$  in zone

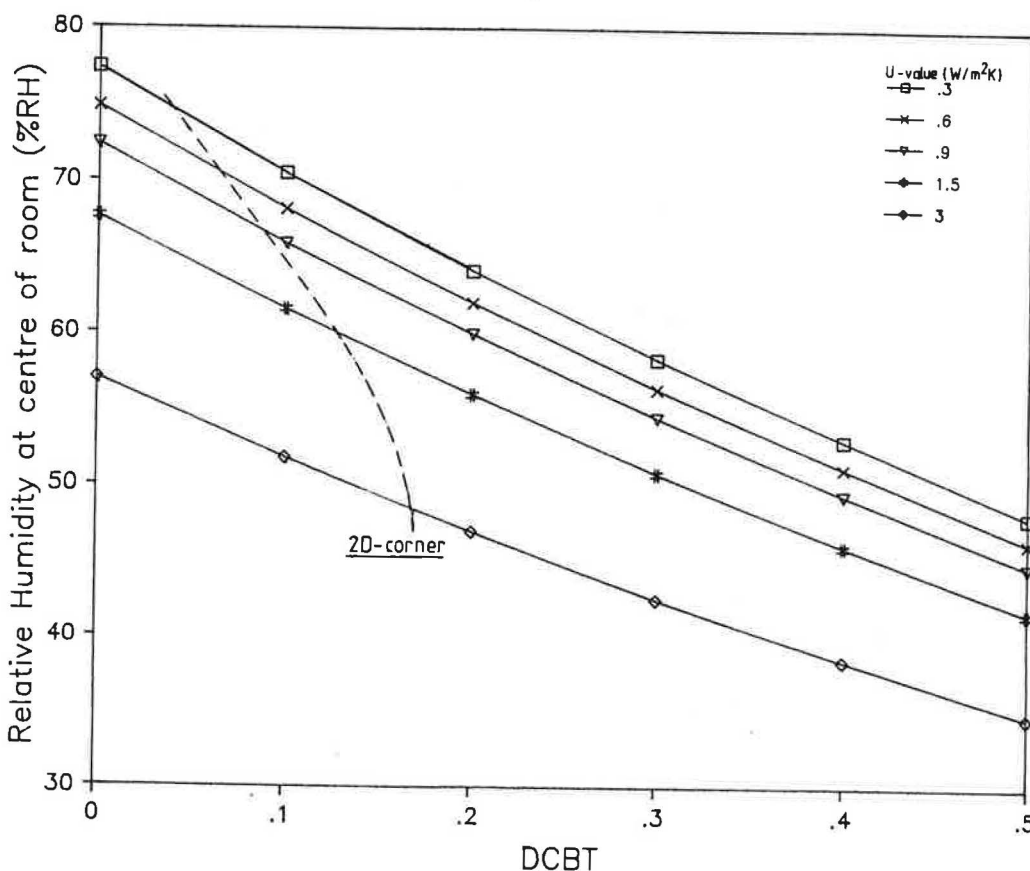
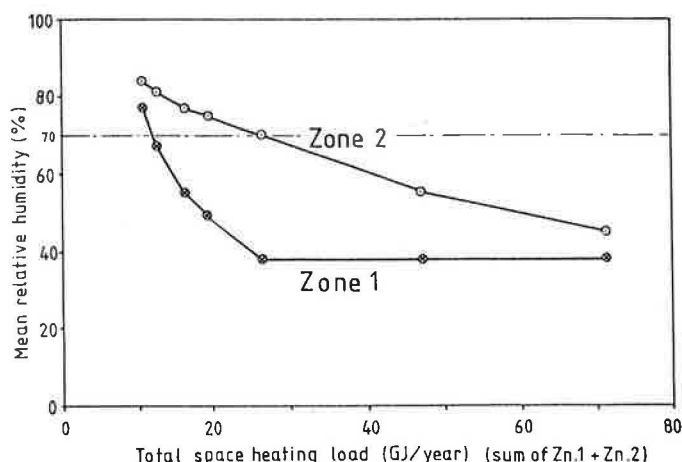


Figure 9 Modelled humidity at the centre of a room to obtain a humidity of 80% at the wall surface for varying DCBT:  $T_i = 21^\circ\text{C}$ ,  $T_o = 6^\circ\text{C}$ ,  $R_{si} = 0.12 \text{ m}^2 \text{ K}^{-1} \text{ W}^{-1}$





**Figure 10** Zone mean internal relative humidity as a function of dwelling annual space heating load for a 4-bedroom flat occupied by a 5-person family<sup>(19)</sup>

2, a space heating load of  $46 \text{ GJ y}^{-1}$ , and a space heating cost of  $\text{£}240 \text{ y}^{-1}$ .

The presence of a cold bridge therefore results in an increase in fuel consumption in order to maintain higher internal temperatures and prevent mould growth. Unfortunately it is often the people who can least afford to pay higher bills who live in accommodation with the most severe cold bridging.

## 7 Conclusions and suggestions for further work

External corners can act as significant cold bridges. For example, in a room with uninsulated walls, double glazing and a 3D corner, the corner temperature may be lower than that of the glazing. This is a result of the geometry of the corner allowing two- and three-dimensional heat flow.

Restricting the flow of air within the corner may further increase the cold bridging by 60% as a result of reduced surface heat transfer. A better understanding of the surface heat transfer in corners is therefore required in order accurately to determine the cold bridging at corners.

As the level of insulation in a wall is increased the DCBT at the corner is reduced and the temperature at the wall and in the corner increases.

For difficult to cure severe cold bridges, a material of high thermal conductivity placed at the surface may be a solution worthy of investigation.

A simple resistance model can be used to predict the DCBT in corners. The model does not, however, show the change in cold bridge temperature with location of insulation within the wall. It is anticipated that other simple resistance models could be used for more complex cold bridge constructions. If not, a catalogue of DCBT for the most common constructions will be produced.

Finite-element modelling agrees well with measured data, although the model may not account for air movement within the cavity. This is to be investigated further by insulating the cavity and repeating the measurements.

Transient effects are found to be important when examining cold bridges as the DCBT is greater when the external temperature rises. Any catalogue of DCBT must therefore also include details about the transient response of the bridge.

Further work is underway to develop a test day to characterise this response. How important these transient effects are for mould growth will not be fully understood until the results of research into the response of mould to transient conditions is known.

The DCBT can be used to predict the maximum relative humidity in the centre of the room to prevent mould growth at the cold bridge. This in turn can be used to calculate the mean internal temperature, and fuel expenditure required to prevent mould growth for any given level of moisture production. Thus, for a specific cold bridge the cost of space heating required to prevent mould growth can be calculated. Such information may prove a useful tool when examining refurbishment options. For example, external cladding and drylining are often the only solutions to many cold bridge problems. The linking of a cold bridge and fuel cost model may provide the basis for an economic argument with which to justify such measures.

## Acknowledgement

This work was carried out with the support of the Science and Engineering Research Council.

## References

- 1 Saunders C H and Cornish J P *Dampness: one week's complaints in five local authorities in England and Wales* (Garston: Building Research Establishment) (1982)
- 2 CIBSE Guide Section A3: Thermal properties of building structures (London: Chartered Institution of Building Services Engineers) (1986)
- 3 *Condensation in dwellings Part 1: A design guide* (London: MPBW/HMSO) (1970)
- 4 Draft revision to British Standard Code of Practice BS5250: *The control of condensation in buildings* (revision of BS5250, 1975) (Milton Keynes: British Standards Institution) (1987)
- 5 Baldwin R Insulation: Beyond the regulations *Building* pp 54–55 (17th July 1987)
- 6 Courtney R High Insulation-Scenario for the future *Proc. Conf. High Insulation: Impact on Buildings and Services Design*, University of Nottingham, March 1987
- 7 Carslaw H S and Jaeger J C *Conduction of Heat in Solids* 2nd edition (Oxford: University Press) (1959)
- 8 Billington N S and Becher P Some two-dimensional heat-flow problems *J. Inst. Heating Ventil. Eng.* 18(183) 297–312 (1950)
- 9 PAFEC Ltd. Strelly Hall, Main St, Strelly, Nottingham
- 10 Ward T I and Anderson B R Personal communication, Building Research Establishment Scottish Laboratory, East Kilbride, Glasgow Ref N 28/82 (February 1982)
- 11 BuØ F O et al *Kuldebroer Energisparing Byggekader* Norges Byggsforskings Institutt Arbeidsrapport 36 (1981)
- 12 Sarkis B L and Letherman K M Heat flow rates and temperature distributions in corners of external walls and non-isothermal surfaces *Building Env.* 22(4) 251–258 (1987)
- 13 Schild E et al *Environmental Physics in Construction: Its Application in Architectural Design* Ed. M Finbow (London: Granada) (1981)
- 14 Gertis K *Condensation in outer wall corners (Tautwasserbildung in Aussenwandecken)* (in German) DAB 15(10) (1983)
- 15 Nevander L E Koldbrygger I Vaggkonstruktioner (Cold bridges in walls) *Byggaestaren* 40(2) 46–53 (1961)
- 16 Yaneske P and Forrest I D The thermal response of rooms with intermittent, forced convective heating *Building Serv. Eng.* 46(1) 13–17 (1978)
- 17 Bravery A F, Grant C and Saunders C H Controlling mould growth in housing *Proc. Unhealthy Housing Conf. University of Warwick*, December 1987
- 18 Saunders C Personal communication (Scottish Building Research Laboratory) (December 1987)
- 19 Boyd D, Cooper P and Oreszczy T Condensation Risk Prediction: Addition of a condensation model to BREDEM *Building Serv. Eng. Res. Technol.* 9(3) 117–125 (1988)